Fast and Dynamically Stable Optimization-based Planning for High-DOF Human-like Robots

Chonhyon Park and Dinesh Manocha
http://gamma.cs.unc.edu/ITOMP/ (Videos included)

***Abstract*— We present a novel optimization-based motion planning algorithm for high degree-of-freedom (DOF) robots. Our approach combines a multi-contact dynamics formulation with optimization-based planning to compute collision-free, smooth and dynamically stable trajectories. Our formulation is general and can handle multiple simultaneous contacts and non-planar surfaces. We highlight the performance of our algorithm in simulated environments on human-like robots with tens of DOFs.**

I. Introduction

Over the last few years, robots with complex shapes and a high number of controllable joints have been increasingly used for various applications. These include highly articulated bipedal humanoid robots (e.g. HRP-4[1] robot with 34 DOFs, and Hubo II[2], with 40 DOFs). This increased complexity of the robots results in two major challenges for motion planning: (1) the high number of degrees-of-freedom (DOFs) increases the dimensionality of both the configuration and the search spaces, thereby increasing the cost of path computation; and (2) only a subset of possible motion are dynamically stable due to the robot's kinematics and shape. As a result, it is a major challenge to efficiently compute a collision-free trajectory for the robot that can satisfy all stability and smoothness constraints.

There is considerable work on motion planning for high-DOF robots. At a broad level, the previous work can be classified into sample-based planners and optimization-based planners. Sample-based planners, which are based on probabilistic roadmaps [1] or rapidly-exploring random trees [2], are relatively easy to implement and can compute collision-free paths in high dimensions. Recent progress on sample-based planner makes it possible to handle some constraints such as path smoothness and dynamic stability [3], [4], [5]. However, it is relatively difficult to guarantee the quality of the trajectories computed by sample-based planners. On the other hand, optimization-based planners compute a trajectory using a continuous formulation of the problem [6], [7], [8], [9]. Different constraints can be formulated as part of the optimization function for trajectory computation, including path-smoothness constraints and collision checking with static and dynamic obstacles.

One key task for motion planning is to ensure that the robot's motion resulting from the planned trajectory satisfies the stability constraints. For example, the computed posture should be statically stable, and the projection of the center of mass of the robot should lie inside the foot-supported polygon; similarly, the zero moment point (ZMP) should lie inside the support polygon [10] for dynamic stability on a flat plane. Some of the current algorithms plan a trajectory that satisfies the ZMP constraint and derive the appropriate hip or torso motion to compute a trajectory. However, the resulting hip or torso motion is often jerky because it has to compensate for the lower-limb motions [11]. In the general case, a robot is dynamically stable when the forces and torques acting on the robot maintain an equilibrium; Newton-Euler equations can be used to compute those forces and torques [12]. Since the contacts between the robot and the obstacles exert forces on the robot, we need to compute the appropriate forces (including their duration) from the contacts as part of overall motion planning.

In this paper, we present an efficient optimization-based planning algorithm to compute dynamically stable, smooth, and collision-free robot motions for high-DOF robots. Our planner minimizes the trajectory cost function, which is composed of cost functions for dynamic stability, calculation of a collision-free path, and path smoothness. We also optimize the durations of the contacts along with the state of the robot, which allows our algorithm to compute a stable motion with multiple contacts. In order to accelerate the computation, we use a hierarchical decomposition of a high-DOF robot and compute the trajectory of low-DOF components in a bottom-up manner. Based on the decomposition, we incrementally compute the trajectory for each node in the hierarchy. Moreover, the trajectories of all the components planned during the prior state are treated as constraints in the optimization formulation for the planning of the subsequent components. We highlight the performance of this model on robots with 20-40 DOFs on non-planar surfaces with multiple contacts. Moreover, we observe considerable speedups over prior optimization-based algorithms.

The rest of the paper is organized as follows. In Section II, we survey related work in motion planning and compare our approach with prior methods. We give an overview of the background algorithms in Section III. In Section IV, we present our planning algorithm, based on dynamic stability constraints. Finally, we highlight our algorithm's performance in simulated environments in Section V.

Chonhyon Park and Dinesh Manocha are with the Department of Computer Science, University of North Carolina at Chapel Hill. E-mail: {chpark, dm}@cs.unc.edu.

[1]http://global.kawada.jp/mechatronics/hrp4.html

[2]http://hubolab.kaist.ac.kr/

II. Related Work

In this section, we give a brief overview of prior work on optimization-based motion planning and motion stability constraints.

A. Optimization-based Motion Planning

The simplest trajectory smoothing algorithms use the shortcut method to smoothen the motion trajectory. These algorithms are used as a postprocess on computed collision-free trajectories; they optimize adjacent pairs of configurations along the computed trajectory, using local planning, to compute smooth paths [13], [14].

Many techniques based on numerical optimization have been proposed in the literature [15]. Khatib proposed the use of potential fields for real-time obstacle avoidance [16]. This approach is extended using elastic strips [17] and elastic bands [18] to compute minimum-energy paths using gradient-descent methods. These methods use a collision-free path as an initial trajectory approximation for the optimization algorithm.

Some recent approaches, such as [6], [7], [19] and [8], directly encode constraints (e.g. the requirement that the path be collision-free and smooth) into the cost functions, then use a numerical solver to compute a trajectory that satisfies all the constraints; these approaches do not require the collision-free initial trajectory, as is the case with prior numerical techniques. Some of these techniques explicitly compute the gradient [6], [19], while others do not [7], [8].

B. Motion Stability Constraints

Ensuring that the computed motion is stable is an important criterion in motion planning for high-DOF robots. There is considerable work on the walking motion of bipedal robots [11]; proper, stable walking motion is essential for humanoid robots. In order to handle motion dynamics, the stability constraint is formulated to maintain the equilibrium among the forces and torques acting on the robot: inertia, Coriolis, gravity, ground-reaction forces from contacts, etc. In this section, we give an overview of the previous motion planning approaches that achieve dynamic stability in their computed motions and compare our algorithm with them.

The zero moment point (ZMP)-based methods compute the projected ZMP in the support polygon based on the assumption that contacts between the robot and the environment happen only on a planar terrain. Furthermore, the standard ZMP-based methods [20], [21], [22] first plan the ZMP trajectory, then (in the case of humanoids) derive the hip or torso motion that will satisfy that trajectory. However, adjusting only hip or torso motion may not be enough to achieve the desired ZMP trajectory, and it may generate jerky motion [11]. The ZMP concept has been extended to wrench space in order to compute motions on non-planar terrains [23], [24]. The wrench-space approaches check whether the sum of wrenches applied on the robot is within the polyhedral convex cone of the convex wrench. The wrenches can be computed even if contacts are placed on different heights. This approach is limited: it can generate motions only when the height of the center of mass (CoM) is constant (due to the assumption used in the algorithm), and it can generate jerky motion under certain circumstances.

Dalibard et al. [5] suggested an approach that first computes a collision-free statically balanced path using sample-based planning algorithms, then transforms the path using small-space controllability of the robot based ZMP [5]. It is a general method for collision-free motions, but still has the limitations of ZMP.

Recently, many approaches have been proposed to include contacts in their optimization formulation [25], [26]. The optimization algorithm directly uses the contact forces and the robot state as variables [27]. This direct optimization generates smooth paths and does not have the limitations of the prior approaches; however, the increased number of optimization variables increases the complexity of the computation and affects planning performance.

Contact-Invariant Optimization (CIO) [28] has been used to generate visually-natural motion for character animation using a simplified physics formulation. This approach optimizes contact variables using contact phases rather than directly optimizing the individual contact forces. It reduces the search space and accelerates the overall performance. Later, CIO is applied to a compute physical lower-limb motions of a humanoid model [29].

III. Background

Our motion planner is built on the ITOMP optimization-based framework [8] and use Contact-Invariant Optimization (CIO) [28] to find a dynamically stable motion. In this section, we give a brief overview of ITOMP and CIO.

A. ITOMP: Incremental Trajectory Optimization

ITOMP is a motion planning algorithm that computes smooth, collision-free paths using optimization techniques. A configuration of a robot $\mathbf{q}$ is determined by all the actuated joints of the robot, as well as by the position and orientation of the robot in the workspace. We denote the trajectory for a robot as a function $M(t)$ for $t \in [0, T]$, where we assume that we know the length of the trajectory T. $M(t)$ is a discretized trajectory composed of $N + 2$ waypoint configurations: $M(t) = \{\mathbf{q}_I, \mathbf{q}_1, ..., \mathbf{q}_N, \mathbf{q}_G\}$, where $\mathbf{q}_k$ is a trajectory waypoint at time $\frac{k}{N+1}T$. $\mathbf{q}_I$ and $\mathbf{q}_G$ represent the given initial and goal configurations, respectively. Given $\mathbf{q}_I$ and $\mathbf{q}_G$, ITOMP generates the initial trajectory by discretizing the configurations along a curve that connect $\mathbf{q}_I$ and $\mathbf{q}_G$ into $N + 1$ segments equally spaced in time.

ITOMP computes a smooth trajectory $M(t)$ that connects the initial and goal configurations of the robot by solving an optimization problem. The optimization algorithm avoids collisions with obstacles using conservative bounds while simultaneously satisfying other constraints. ITOMP optimizes the positions of internal waypoints $\{\mathbf{q}_1, ..., \mathbf{q}_N\}$ by optimizing the following cost function:

$$\min_{\mathbf{q}_1,...,\mathbf{q}_N} \sum_{k=1}^{N} (C_{Obs}(\mathbf{q}_k) + C_{Spec}(\mathbf{q}_k) + \|\mathbf{q}_{k-1} - 2\mathbf{q}_k + \mathbf{q}_{k+1}\|^2), \quad (1)$$

where the cost terms $C_{Obs}(\cdot)$, and $C_{Spec}(\cdot)$ represent the obstacle cost and the problem-specific additional constraints, respectively. $\sum_{k=1}^{N} \|\mathbf{q}_{k-1} - 2\mathbf{q}_k + \mathbf{q}_{k+1}\|^2$ represents the smoothness of the entire trajectory, which is computed by the sum of squared accelerations along the trajectory.

The optimization problem in (1) computes a local or global optimal trajectory of the robot configuration waypoints $\mathbf{q}_i$. In order to improve robot's responsiveness and safety in dynamic environments, ITOMP uses a replanning approach to compute collision-free paths amongst dynamic obstacles. Using estimations of the trajectories of moving obstacles over a short time horizon, ITOMP computes conservative bounds on the position of the obstacles over a short time interval.

B. Contact-Invariant Optimization

In order to compute a physically correct, stable motion, the intermittent contacts between the robot and the environment during the motion trajectory should be planned. For example, a simple walking motion for a humanoid robot requires planning both when a foot is on the ground and when it is not in contact with the ground, and this computation must be performed for each foot. Some earlier approaches [20] use pre-defined positions for footsteps to simplify the problem, but this works only in limited cases where the footsteps are uniform and symmetric.

We use the Contact-Invariant Optimization (CIO) approach. In this formulation, the robot has several potential contact points (e.g. feet or hands), that can make contacts with the obstacles in the environment. It is assumed that both the robot links and obstacles are rigid, and that each contact point has dry friction. In optimization-based planning, additional contact-related variables for the potential contact points need to be optimized along with the trajectory waypoints to determine when the corresponding contacts exist in the computed trajectory.

The CIO approach introduces *contact phases*. Instead of defining the contact-related variables as a trajectory with N waypoint values, we can approximate the trajectory with fewer P values, where P is the number of contact phases and $P < N$. The trajectory of contact-related variables is defined as $\mathbf{a}^l = \{a_1^l, ..., a_P^l\}$ for l-th potential contact point, and a map $\rho(k) = p$ is used to retrieve the corresponding contact variable a_p^l for a waypoint $\mathbf{q}_k$. This approach assumes that the contacts are invariant in a contact phase. It reduces the number of variables, a_p^l, that are used during the optimization algorithm. A large value of a_p^l implies that the contact l must be active during the phase p; for a small a_p^l, the contact l can be ignored.

For a waypoint $\mathbf{q}_k$, the CIO approach computes the stability cost by using two sub-cost functions:

$$C_{Stability}(\mathbf{q}_k) = C_{Physics}(\mathbf{q}_k) + C_{Contact}(\mathbf{q}_k). \quad (2)$$

$C_{Physics}(\cdot)$ represents the cost due to the violation of the balance, and $C_{Contact}(\cdot)$ represents the cost of the violation of contacts. The contact invariant cost $C_{Contact}(\cdot)$ is defined as

$$C_{Contact}(\mathbf{q}_k) = \sum_{l=1}^{L} \sum_{k=1}^{N} a_{\rho(k)}^l (\|\mathbf{e}_k^l(\mathbf{q}_k)\|^2 + \|\dot{\mathbf{c}}_k^l(\mathbf{q}_k)\|^2), \quad (3)$$

where L is the total number of potential contact points, and $\mathbf{e}_k^l$ and $\dot{\mathbf{c}}_k^l$ are the contact-violation vector and the velocity of the l-th contact point at a waypoint $\mathbf{q}_k$, respectively. $\mathbf{e}_k^l$ is a 4D vector that concatenates the 3D position and normal angle differences between the l-th contact point and the nearest point on an obstacle. Therefore, $\mathbf{e}_k^l$ represents the misalignment between the l-th potential contact point on the robot and the nearest point on the environment in both position and orientation. If $a_{\rho(k)}^l$ is large, the misalignment of the l-th contact makes the cost function very high, while the misalignment of small $a_{\rho(k)}^l$ does not result in significant cost. $\dot{\mathbf{c}}_k^l$ for a large value of $a_{\rho(k)}^l$ corresponds to slip of the contact point.

The cost of $C_{Contact}(\mathbf{q}_k)$ corresponds to the global minimum when all $\mathbf{a}_{\rho(k)}$ are zero. However, these cases are prevented by the second cost term $C_{Physics}(\mathbf{q}_k)$, which represents the cost that penalizes for the violation of the equilibrium of forces and torques. If the contact variables $\mathbf{a}_{\rho(k)}$ have small values, it increases the cost of $C_{Physics}(\mathbf{q}_k)$ as described in Section IV-C.

IV. Motion Planning with Dynamic Stability

In this section, we present the details of our approach that computes a collision-free, smooth trajectory that maintains the robot's dynamic stability. We first present the trajectory optimization function. Next, we introduce the underlying physics-based formulation of the cost computation and describe the overall algorithm.

A. Optimization with Stability Cost

Based on the ITOMP cost function (1), our planning algorithm uses CIO to compute a dynamically stable trajectory for robots. Based on CIO, our new optimization formulation is:

$$\min_{\substack{\mathbf{q}_1,...,\mathbf{q}_N,\\ \mathbf{a}_1,...\mathbf{a}_P}} \sum_{k=1}^{N} (C_{Obs}(\mathbf{q}_k) + C_{Stability}(\mathbf{q}_k, \mathbf{a}_{\rho(k)}) + \|\mathbf{q}_{k-1} - 2\mathbf{q}_k + \mathbf{q}_{k+1}\|^2), \quad (4)$$

where $1 \leq \rho(k) \leq P$, and $\mathbf{a}_i = \left[a_i^1, ..., a_i^L\right]$, the vector of contact variables of L potential contact points for phase i. In our objective function (4), $C_{Stability}(\mathbf{q}_k)$ is the stability cost for the waypoint $\mathbf{q}_k$, which is defined in Equation (2). Though [28] uses a simplified physics model to make animated characters move naturally, we compute $C_{Physics}(\mathbf{q}_k)$ accurately based on Newton-Euler equations.

B. Dynamic Stability Computation

A key issue in our formulation is computation of physics-violation cost $C_{Physics}(\mathbf{q}_k)$ for maintaining dynamic stability (as shown in Equation (2)). We first describe our physics-based formulation. Fig. 1(a) illustrates a high-DOF human-like robot, which makes contacts with the ground plane

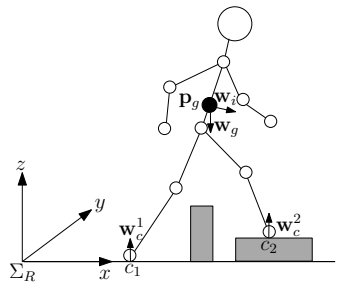

(a) Wrenches exert on the robot.

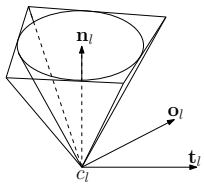

(b) Friction cone and approximating pyramid.

Fig. 1: A humanoid robot makes contacts c_1 and c_2 with the ground plane. The gravity wrench $\mathbf{w}_g$ and the inertia wrench $\mathbf{w}_i$ are applied to the robot. The contact wrenches $\mathbf{w}_c^1$ and $\mathbf{w}_c^2$ can have values in their friction cone. The robot is stable when $\mathbf{w}_c^1 + \mathbf{w}_c^2 + \mathbf{w}_g + \mathbf{w}_i = \mathbf{0}$.

using its feet. Let Σ_R be the global coordinate frame, J be the number of links in the robot, and $c_1, ..., c_L$ be the positions of L contact points. There are several wrenches (forces and torques) exerted on the robot. The robot is dynamically stable when all wrenches on the robot constitute an equilibrium [12].

1) Contact wrench : The sum of contact wrenches $\mathbf{w}_c^l$ applied to the robot from contact points c_l with respect to Σ_R is given by

$$\mathbf{w}_c = \sum_{l=1}^{L} \mathbf{w}_c^l = \sum_{l=1}^{L} \begin{bmatrix} \mathbf{f}_l \\ \mathbf{r}_l \times \mathbf{f}_l \end{bmatrix}, \tag{5}$$

where $\mathbf{f}_l$ is the contact force of c_l and $\mathbf{r}_l$ is the position vector of c_l in the frame Σ_R. Coulomb's friction law stipulates that $\mathbf{f}_l$ should be constrained in its friction cone F_l to avoid any slipping motion. This constraint can be formulated as:

$$f_{lt}^2 + f_{lo}^2 \leq \mu f_{ln}^2, \tag{6}$$

where $\begin{bmatrix} \mathbf{f}_{ln} & \mathbf{f}_{lt} & \mathbf{f}_{lo} \end{bmatrix}^T$ corresponds to $\mathbf{f}_l$, with respect to the frame of c_l, which is defined by the axes of the contact normal $\mathbf{n}_l$, $\mathbf{t}_l$ and $\mathbf{o}_l$ that satisfy $\mathbf{n}_l \times \mathbf{t}_l = \mathbf{o}_l$. Our formulation of $\mathbf{w}_c$ considers the contact normal and the friction coefficient. This makes it general enough for uneven ground surface, unlike prior approaches based on ZMP.

2) Gravity wrench : The gravity wrench $\mathbf{w}_g$ is

$$\mathbf{w}_g = \begin{bmatrix} M\mathbf{g} \\ \mathbf{p}_g \times M\mathbf{g} \end{bmatrix}, \tag{7}$$

where $\mathbf{p}_g$ is the center of mass (CoM) of the robot. $\mathbf{p}_g$ can be computed by $\sum_{j=1}^{J} m_j \mathbf{p}_j / \sum_{j=1}^{J} m_j$, where m_j and $\mathbf{p}_j$ are the mass and the position of j-th link of the robot in Σ_R, respectively. Here $\mathbf{g}$ is $\begin{bmatrix} 0 & 0 & -g \end{bmatrix}^T$.

3) Inertia wrench : The inertia wrench $\mathbf{w}_i$ can be written as

$$\mathbf{w}_i = \begin{bmatrix} M\ddot{\mathbf{p}}_g \\ \mathbf{p}_g \times M\ddot{\mathbf{p}}_g - \dot{\mathcal{L}} \end{bmatrix}, \tag{8}$$

where $\mathcal{L}$ is the angular momentum of the robot with respect to $\mathbf{p}_g$ is defined as

$$\mathcal{L} = \sum_{j=1}^{J} \left[m_j (\mathbf{p}_j - \mathbf{p}_g) \times \dot{\mathbf{p}}_j + I_j \boldsymbol{\omega}_j \right], \tag{9}$$

where I_j and $\boldsymbol{\omega}_j$ are the inertia tensor and the angular velocity of the j-th link of the robot, respectively.

The robot is dynamically stable when it satisfies

$$\mathbf{w}_c + \mathbf{w}_g + \mathbf{w}_i = \mathbf{0}. \tag{10}$$

C. Computation of Physics Violation Cost

Next we describe the computation of the physics-violation cost $C_{Physics}(\mathbf{q}_k)$ in (2). First we formulate the combination of contact forces, which can be defined as:

$$\mathbf{f} = [\mathbf{f}_1^T, ..., \mathbf{f}_L^T]^T. \tag{11}$$

Equation (5) can be represented as $\mathbf{w}_c = \mathbf{B}\mathbf{f}$, where $\mathbf{B}$ is the corresponding $6 \times 3L$ matrix. Using this formulation, we solve an inverse dynamics computation problem, which computes $\mathbf{f}$ such that it satisfies the Coulomb friction constraints of Equation (6):

$$\mathbf{f} = \arg\min_{\mathbf{f}^*} (\|\mathbf{B}\mathbf{f}^* + \mathbf{w}_g + \mathbf{w}_i\| + \mathbf{f}^{*T}\mathbf{R}\mathbf{f}^*). \tag{12}$$

The Coulomb friction constraint is usually converted to an inequality constraints, using a pyramid to approximate a friction cone F_i (shown in Fig. 1(b). The constraint for $\mathbf{f}_i$ is reduced to

$$\begin{aligned} -\mu f_{ln} \leq f_{lt} \leq \mu f_{ln} \\ -\mu f_{ln} \leq f_{lo} \leq \mu f_{ln}. \end{aligned} \tag{13}$$

In (12), we add the contact variable penalty term $\mathbf{f}^{*T}\mathbf{R}\mathbf{f}^*$ as it is used in [28]. It increases the difference between $\mathbf{f}$ from (12) and the actual optimal force that satisfies (10), when contact variable $\mathbf{a}^l$ is small for a large contact force $\mathbf{f}_i$. The matrix $\mathbf{R}$ is a $3L \times 3L$ diagonal matrix, and its diagonal elements correspond to

$$\mathbf{R}_{jj} = \frac{k_0}{(a^l_{\rho(k)})^2 + k_1}, \tag{14}$$

where $3l - 2 < j < 3l$. k_0 and k_1 are constants that control the weight of the penalty cost.

The quadratic programming (QP) problem (12) can be solved using a QP solver; the result value of $\mathbf{f}$ is used to compute the $C_{Physics}(\mathbf{q}_k)$, which is evaluated as

$$C_{Physics}(\mathbf{q}_k) = \|\mathbf{B}(\mathbf{q}_k)\mathbf{f} + \mathbf{w}_g(\mathbf{q}_k) + \mathbf{w}_i(\mathbf{q}_k)\|. \tag{15}$$

If there are more potential contact points on the robot (e.g. hips), Equation (12) can compute the contact reaction forces of all contact points, while Equation (3) generates penalty forces for violation of contacts.

	Robot DOFs # Contacts	Iterations	Planning Time(s)	Trajectory Smoothness
Benchmarks		Mean (Std. Dev.)		
Steps (Fig. 2)	34 2	140.27 (22.667)	17.467 (3.325)	10.315 (2.975)
Obstacles (Fig. 3)	34 2	68.11 (162.749)	10.213 (24.863)	5.626 (4.021)
Door (Fig. 4)	34 3	35.64 (15.272)	4.404 (1.419)	4.419 (1.789)
Drawer (Fig. 5)	34 3	73.954 (143.026)	13.054 (19.868)	0.579 (0.097)

TABLE I: Planning results for different benchmarks on a single CPU core. We highlight the robot DOFs and the number of potential contact points with the environment. We measure the means and the standard deviations for the number of iterations in the numerical optimization process; the planning time needed to compute the first collision-free solution; and the smoothness of the trajectory for different benchmarks. The smoothness is computed by the sum of joint accelerations at the trajectory waypoints for all active joints, which means that trajectories with lower values are smoother.

V. Results

In this section, we highlight the performance of our planning algorithm in simulated environments. We have implemented our algorithm in a simulator with a human-like robot model which has 34 DOFs.

We highlight the results for motion planning in different environments for the robot in Table I. We compute the trajectories of the robot in two environments, where the robot must move by walking from the initial configuration to the goal configuration. We evaluate the performance in two scenarios, where the robot needs to make contacts using its hand with the environments. We measure three components to evaluate the performance: the number of iterations in the optimization routines; the planning time to find the first collision-free and stable solution; and the smoothness of the trajectory. The results, shown in Table I, are the averages and standard deviations of 100 trials for each scenario. Videos of these and other benchmark experiments can be found at http://gamma.cs.unc.edu/ITOMP/.

We use hierarchical planning in our benchmarks to improve the planning performance. Hierarchical planning is a divide-and-conquer approach that decomposes a high-dimensional planning problem into several lower-dimensional problems [30], [31]. We decompose a robot into 5 different components: a lower body, which includes legs and pelvis; a torso; a head; a left arm; and a right arm, then incrementally plan the trajectory of the robot using this decomposition. In Fig. 2-5, different robot components used in hierarchical planning are marked with different colors.

Parameter values used our experiments are: N (Number of waypoints) = 100, P (Number of contact phases) = 5, k_0, k_1 (Contact variable penalty terms) = 0.01, 0.001, r (local displacement vector) = 0.1, T (length of the motion)=5.

Our first benchmark is planning a trajectory on an uneven terrain. The height of the terrain varies such that the ZMP-based methods may not be able to compute a dynamically stable solution. The planners with stability constraints compute the contact points between the robot's feet and the terrain, and place the robot feet on these points. This generates a walking motion towards the goal configuration while satisfying the stability requirements. Fig. 2 shows the trajectory computed by the dynamic stability constraint.

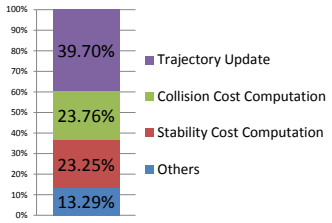

Fig. 6: Timing breakdown of an iteration of the trajectory optimization.

In our second benchmark, the environment consists of several obstacles that the robot needs to avoid. We place an obstacle on the ground that the robot cannot go around, forcing it to pass over the obstacle. The trajectory computed with the stability constraint is shown in Fig. 3. In the computed trajectory, the robot does not collide with the obstacles and passes over the obstacles on the ground.

In the next two benchmarks, we test our algorithm with with scenarios where the robot makes additional contacts with its right hand, while satisfying the stability constraints. The robot exerts force on the objects in the environment to perform manipulation tasks. In the third benchmark, the robot pushes a door (Fig. 4) to reach a goal. The robot pulls a drawer (Fig. 5) to move it to the desired position in the last benchmark.

Fig. 6 highlights the timing breakdown of an iteration of the trajectory computation. The percentage of time spent in stability cost computation takes 23.2% of the total computation time.

Algorithms	Collision -aware	Dynamic Stability	Uneven Terrain	Smooth Motion	Vertical movement of CoM	Physically Correct Model
ZMP-based [20], [21]	✗	✓	✗	✗	✓	✓
Stability Computation in Wrench Space [23]	✗	✓	✓	✗	✗	✓
Transform from Statically Balanced Path [5]	✓	✓	✗	✓	✓	✓
Contact-Invariant Optimization [28]	✓	✓	✓	✓	✓	✗
Direct Contact Force Optimization [27]	✓	✓	✓	✓	✓	✓
Our Approach	✓	✓	✓	✓	✓	✓

TABLE II: This table compares the feature of our motion planning with dynamic stability algorithm with other approaches. Our approach can handle all the constraints, similar to the direct contact force optimization algorithm [27], but is an order of magnitude faster.

Comparisons: Our algorithm combines the CIO approach and the wrench-space stability computation, integrating them into a hierarchical optimization framework. Our approach can compute smooth, physically-correct motions while efficiently computing the motions and reactions resulting from various contacts. Our approach is more than an order of magnitude faster than the other planning algorithms described above ([5], [28], [27]). At the same time, other planners with close to real-time performance either do not perform obstacle-aware motion planning or do not provide similar guarantees on dynamic stability. Table II shows a summary of the capabilities of the different algorithms.

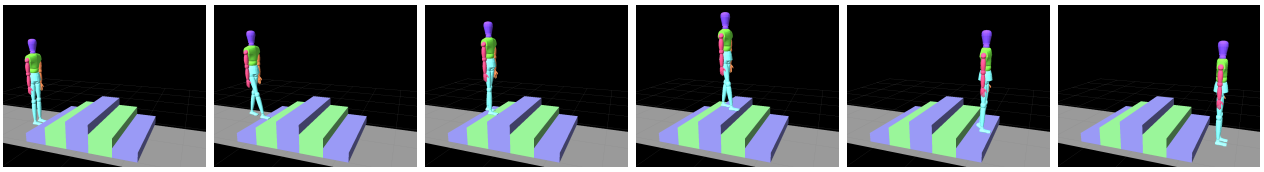

Fig. 2: Snapshots of the computed trajectory planned across uneven terrain of varying heights. The proper footstep points are computed during the optimization, and the entire walking motion trajectory is dynamically stable.

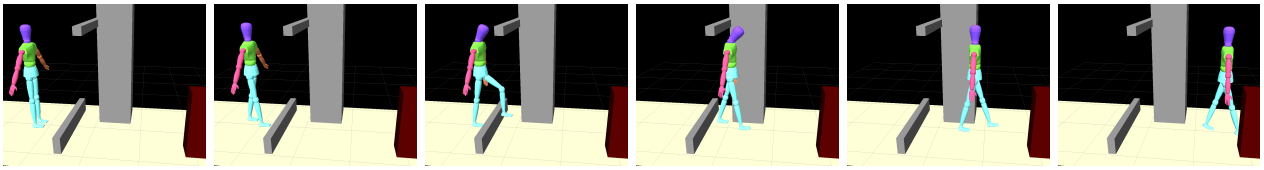

Fig. 3: Snapshots of the computed trajectory for the environment with obstacles. There is an obstacle between the initial position and the goal position that the robot cannot detour around. The computed trajectory passes over the obstacle.

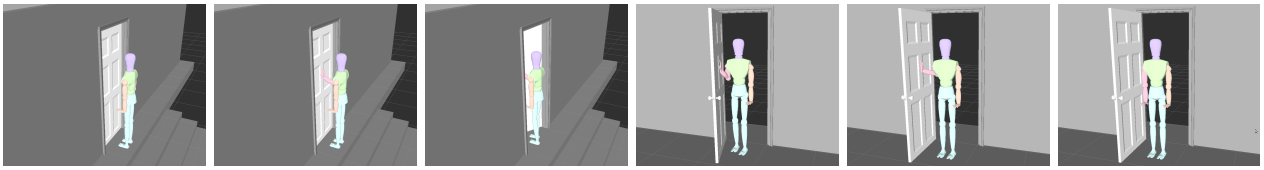

Fig. 4: We highlight the smooth and dynamic stable trajectory computed by our planner to perform the specific tasks. The robot uses multiple degrees of freedom, including 14 DOF on the legs to move and 7 DOF on the arm to open the door.

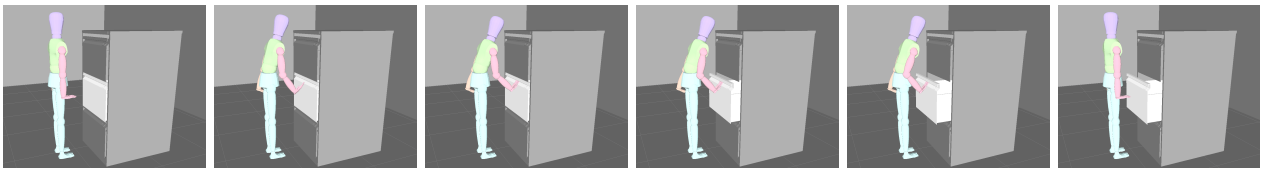

Fig. 5: We highlight the high-DOF trajectory for the robot to perform the tasks for opening the drawer by our algorithm.

VI. Conclusions, Limitations and Future Work

We present a fast, dynamically stable, optimization-based motion planning algorithm for high-DOF robots. We use contact variables to compute dynamically stable motions. The stability of the motion is computed in a wrench space, and we compute the friction force that creates an equilibrium between the forces exerted on the robot. Our formulation of contacts is general and can handle multiple contacts simultaneously. We highlight the performance of our algorithm using a human-like robot with 34 DOFs.

There are some limitations to our approach. Currently, our approach (like the previous ITOMP [8] and CIO [28] approaches) assumes a fixed length of motion. This length of motion could be optimized in the future. Also, our formulation uses discretized waypoints on the continuous trajectory and the computation is only performed on the waypoints. However, the error due to the small interval is small and can be easily corrected with a real-time control approaches [11], [22]. For a feasible trajectory computed by optimization-based planner, a controller can be used to provide a feedback according to the measured executed trajectory.

There are many avenues for future work. Recently, we have extended our approach on more complex benchmarks where multiple robots and obstacles exist [32]. Furthermore, we would like to investigate other optimization techniques to improve optimization performance.

VII. Acknowledgments

This research is supported in part by ARO Contract W911NF-10-1-0506, NSF awards 1000579, 1117127 and 1305286, and a grant from Sandia Labs.

References

[1] L. Kavraki, P. Svestka, J. C. Latombe, and M. Overmars, "Probabilistic roadmaps for path planning in high-dimensional configuration spaces," *IEEE Transactions on Robotics and Automation*, vol. 12, no. 4, pp. 566–580, 1996.

[2] J. Kuffner and S. LaValle, "RRT-connect: An efficient approach to single-query path planning," in *Proceedings of IEEE International Conference on Robotics and Automation*, 2000, pp. 995 – 1001.

[3] M. Stilman, "Global manipulation planning in robot joint space with task constraints," *Robotics, IEEE Transactions on*, vol. 26, no. 3, pp. 576–584, 2010.

[4] D. Berenson, S. Srinivasa, and J. Kuffner, "Task space regions a framework for pose-constrained manipulation planning," *The International Journal of Robotics Research*, vol. 30, no. 12, pp. 1435–1460, 2011.

[5] S. Dalibard, A. El Khoury, F. Lamiraux, A. Nakhaei, M. Taıx, and J.-P. Laumond, "Dynamic walking and whole-body motion planning for humanoid robots: an integrated approach," *The International Journal of Robotics Research*, 2013.

[6] N. Ratliff, M. Zucker, J. A. D. Bagnell, and S. Srinivasa, "CHOMP: Gradient optimization techniques for efficient motion planning," in *Proceedings of International Conference on Robotics and Automation*, 2009, pp. 489–494.

[7] M. Kalakrishnan, S. Chitta, E. Theodorou, P. Pastor, and S. Schaal, "STOMP: Stochastic trajectory optimization for motion planning," in *Proceedings of IEEE International Conference on Robotics and Automation*, 2011, pp. 4569–4574.

[8] C. Park, J. Pan, and D. Manocha, "ITOMP: Incremental trajectory optimization for real-time replanning in dynamic environments," in *Proceedings of International Conference on Automated Planning and Scheduling*, 2012.

[9] M. Zucker, N. Ratliff, A. D. Dragan, M. Pivtoraiko, M. Klingensmith, C. M. Dellin, J. A. Bagnell, and S. S. Srinivasa, "CHOMP: Covariant hamiltonian optimization for motion planning," *International Journal of Robotics Research*, 2012.

[10] M. Vukobratovic and D. Juricic, "Contribution to the synthesis of biped gait," *IEEE Transactions on Biomedical Engineering*, no. 1, pp. 1–6, 1969.

[11] Y. Xiang, J. S. Arora, and K. Abdel-Malek, "Physics-based modeling and simulation of human walking: a review of optimization-based and other approaches," *Structural and Multidisciplinary Optimization*, vol. 42, no. 1, pp. 1–23, 2010.

[12] J. C. Trinkle, J.-S. Pang, S. Sudarsky, and G. Lo, "On dynamic multi-rigid-body contact problems with coulomb friction," *ZAMM-Journal of Applied Mathematics and Mechanics*, vol. 77, no. 4, pp. 267–279, 1997.

[13] P. Chen and Y. Hwang, "Sandros: a dynamic graph search algorithm for motion planning," *IEEE Transactions on Robotics and Automation*, vol. 14, no. 3, pp. 390–403, jun 1998.

[14] J. Pan, L. Zhang, and D. Manocha, "Collision-free and curvature-continuous path smoothing in cluttered environments," in *Proceedings of Robotics: Science and Systems*, 2011.

[15] J. T. Betts, "Practical methods for optimal control and estimation using nonlinear programming," in *Advances in design and control*. Siam, 2001, vol. 3.

[16] O. Khatib, "Real-time obstacle avoidance for manipulators and mobile robots," *International Journal on Robotics Research*, vol. 5, no. 1, pp. 90–98, 1986.

[17] O. Brock and O. Khatib, "Elastic strips: A framework for motion generation in human environments," *International Journal of Robotics Research*, vol. 21, no. 12, pp. 1031–1052, 2002.

[18] S. Quinlan and O. Khatib, "Elastic bands: connecting path planning and control," in *Proceedings of IEEE International Conference on Robotics and Automation*, 1993, pp. 802–807 vol.2.

[19] A. Dragan, N. Ratliff, and S. Srinivasa, "Manipulation planning with goal sets using constrained trajectory optimization," in *Proceedings of IEEE International Conference on Robotics and Automation*, 2011, pp. 4582–4588.

[20] Q. Huang, K. Yokoi, S. Kajita, K. Kaneko, H. Arai, N. Koyachi, and K. Tanie, "Planning walking patterns for a biped robot," *IEEE Transactions on Robotics and Automation*, vol. 17, no. 3, pp. 280–289, 2001.

[21] S. Kajita, F. Kanehiro, K. Kaneko, K. Fujiwara, K. Harada, K. Yokoi, and H. Hirukawa, "Biped walking pattern generation by using preview control of zero-moment point," in *IEEE International Conference on Robotics and Automation*, 2003, pp. 1620–1626.

[22] L. Saab, O. E. Ramos, F. Keith, N. Mansard, P. Soueres, and J. Fourquet, "Dynamic whole-body motion generation under rigid contacts and other unilateral constraints," *Robotics, IEEE Transactions on*, vol. 29, no. 2, pp. 346–362, 2013.

[23] H. Hirukawa, S. Hattori, K. Harada, S. Kajita, K. Kaneko, F. Kanehiro, K. Fujiwara, and M. Morisawa, "A universal stability criterion of the foot contact of legged robots-adios zmp," in *IEEE International Conference on Robotics and Automation*, 2006, pp. 1976–1983.

[24] Y. Zheng, M. C. Lin, D. Manocha, A. H. Adiwahono, and C.-M. Chew, "A walking pattern generator for biped robots on uneven terrains," in *Intelligent Robots and Systems (IROS), 2010 IEEE/RSJ International Conference on*. IEEE, 2010, pp. 4483–4488.

[25] G. Schultz and K. Mombaur, "Modeling and optimal control of human-like running," *Mechatronics, IEEE/ASME Transactions on*, vol. 15, no. 5, pp. 783–792, 2010.

[26] H. Dai and R. Tedrake, "Optimizing robust limit cycles for legged locomotion on unknown terrain," in *IEEE Conference on Decision and Control*, 2012, pp. 1207–1213.

[27] M. Posa and R. Tedrake, "Direct trajectory optimization of rigid body dynamical systems through contact," in *Algorithmic Foundations of Robotics X*. Springer, 2013, pp. 527–542.

[28] I. Mordatch, E. Todorov, and Z. Popović, "Discovery of complex behaviors through contact-invariant optimization," *ACM Transactions on Graphics (TOG)*, vol. 31, no. 4, p. 43, 2012.

[29] I. Mordatch, J. M. Wang, E. Todorov, and V. Koltun, "Animating human lower limbs using contact-invariant optimization," *ACM Transactions on Graphics (TOG)*, vol. 32, no. 6, p. 203, 2013.

[30] O. Brock and L. E. Kavraki, "Decomposition-based motion planning: a framework for real-time motion planning in high-dimensional configuration spaces," in *IEEE International Conference on Robotics and Automation*, 2001, pp. 1469–1474.

[31] L. Zhang, J. Pan, and D. Manocha, "Motion planning of human-like robots using constrained coordination," in *IEEE-RAS International Conference on Humanoid Robots*, 2009, pp. 188–195.

[32] C. Park and D. Manocha, "Smooth and dynamically stable navigation of multiple human-like robots," in *Algorithmic Foundations of Robotics XI*. Springer, 2014.